Near-Infrared Spectroscopy of Faint Companions around Young Stellar Objects Associated with the Taurus Molecular Cloud

Itoh, Yoichi ; Tramura, Motohide ; Hayashi, Masahiko ; Oasa, Yumiko ; Hayashi, Saeko S. ; Fukagawa, Misato ; Kudo, Tomoyuki ; Mayama, Satosh…

(Citation)
Publications of the Astronomical Society of Japan,60(2):209-218

(Issue Date)
2008-04-25

(Resource Type)
journal article

(Version)
Version of Record

(URL)
https://hdl.handle.net/20.500.14094/90001427

PASJ: Publ. Astron. Soc. Japan **60**, 209–218, 2008 April 25

Near-Infrared Spectroscopy of Faint Companions around Young Stellar Objects Associated with the Taurus Molecular Cloud*

Yoichi ITOH,[1] Motohide TAMURA,[2] Masahiko HAYASHI,[3,4]
Yumiko OASA,[1] Saeko S. HAYASHI,[3,4] Misato FUKAGAWA,[5] Tomoyuki KUDO,[4]
Satoshi MAYAMA,[4] Miki ISHII,[3] Tae-Soo PYO,[3] Takuya YAMASHITA,[3†] and Junichi MORINO[2]
[1]*Graduate School of Science, Kobe University, 1-1 Rokkodai, Nada-ku, Kobe 657-8501*
yitoh@kobe-u.ac.jp
[2]*National Astronomical Observatory, 2-21-1 Osawa, Mitaka, Tokyo 181-8588*
[3]*Subaru Telescope, National Astronomical Observatory of Japan, 650 North A'ohōkū Place, Hilo, HI 96720, USA*
[4]*School of Mathematical and Physical Science, Graduate University for Advanced Studies (Sokendai), 2-21-1 Osawa, Mitaka, Tokyo 181-8588*
[5]*Graduate School of Science, Nagoya University, Furo-cho, Chikusa-ku, Nagoya 464-8601*

(Received 2007 July 19; accepted 2007 November 7)

Abstract

We have conducted near-infrared spectroscopy of 26 faint objects around young stellar objects in the Taurus molecular cloud. These objects were detected during a course of near-infrared coronagraphic searches for companions around 72 young stellar objects with the Subaru Telescope and the near-infrared coronagraph CIAO (coronagraphic imager with adaptive optics). A comparison of the Subaru and HST archive images revealed that three central stars and faint companions share common proper motions, suggesting that they are physically associated with each other. None of the 26 sources show deep water absorption bands at near-infrared, except for DH Tau B. This result indicates that all of them, but DH Tau B, have a high photospheric temperature or a large amount of excess from circumstellar materials.

Key words: planetary systems: formation — techniques: high angular resolution

1. Introduction

Searches for extrasolar planets have been successful so far in finding more than 200 planet candidates, with their physical characteristics being much different from those in our solar system. Many systems show that massive gaseous planets orbit close to their central stars, whereas planetary orbits are highly eccentric in other cases. The current samples of extrasolar planets, however, are biased toward those with small orbital radii, more than half of them having semimajor axes of < 1 AU, as a result of detection methods that have higher sensitivity to objects orbiting closer to the central stars. A comprehensive view of extrasolar planetary systems including bodies with large orbital radii is yet to be revealed.

Direct imaging of extrasolar planets, on the other hand, has higher sensitivities for larger orbital radii. The dynamic range of imaging required to detect a gas giant is extremely high, such as 10^9 for Jupiter against the Sun in the optical and near-infrared wavelengths. However, this range is significantly reduced if a planetary system is younger. For example, a 10-Jupiter mass ($10 M_{\rm J}$) planet has a luminosity greater than $10^{-4}\ L_\odot$ if it is younger than 10^7 yr (Burrows et al. 1997). Such young systems are located relatively faraway (~ 100 pc) compared with the more evolved stars in the solar neighborhood (~ 10 pc), but still in the detectable range with a telescope in the 8–10 m class combined with an adaptive optics (AO) system if their orbital radii are larger than ~ 10 AU. In fact, a few detections of marginal planet candidates, or planet-brown dwarf boundary-mass objects were so far reported in some favorable cases (e.g., 2M 1207: Chauvin et al. 2005a; GQ Lup: Neuhäuser et al. 2005; AB Pic: Chauvin et al. 2005b; CHXR 73: Luhman et al. 2006, and see below for DH Tau).

As one of the key programs of the Subaru Telescope, a near-infrared coronagraphic survey was conducted for protoplanetary disks and faint companions around young stellar objects (YSOs) in the nearby clouds. The survey targets mostly consisted of classical and weak-emission T Tauri stars and Herbig Ae stars in the Taurus–Auriga molecular clouds, including 12 stars whose disks were already detected at the millimeter wavelengths (Kitamura et al. 2003).

During the course of the survey, a companion to the classical T Tauri star DH Tau was detected showing a common proper motion when the survey image was compared with the HST archive optical images. This object, DH Tau B, was claimed to be a young brown dwarf with an effective temperature of 2700–2800 K (Itoh et al. 2005), which was derived by comparing its 1–2.5 μm spectral energy distribution (SED) and K I and Na I line equivalent widths with those of the synthetic spectra of very low-mass objects (Tsuji et al. 2004). The mass of DH Tau B was estimated to be 30–50 $M_{\rm J}$ from its luminosity and the effective temperature plotted on the evolutionary tracks (D'Antona et al. 1997; Baraffe et al. 2003).

In this paper, we present the results of near-infrared spec-

* Based on data collected at the Subaru Telescope, which is operated by the National Astronomical Observatory of Japan.

† Present address: Astrophysical Science Center, Hiroshima University, 1-3-1 Kagamiyama, Higashi-Hiroshima, Hiroshima 739-8526.

troscopy of 26 faint companion candidates in the Taurus molecular cloud as well as a "proper-motion test" similar to that of Itoh et al. (2005). These companion candidates were found with the "self-subtraction" image reduction method, which preferentially detects pointlike sources and is not sensitive to an extended circumstellar structure, about which the results will be presented elsewhere.

2. Observations and Data Reduction

The Subaru disk and planet search (SDPS) program was conducted for 18 nights from 2002 to 2004 while searching for scattering disk emission and faint companions in the H-band. Seventy-two targets were selected from YSOs associated with the Taurus molecular cloud. The near-infrared coronagraph camera CIAO (Tamura et al. 2000; Murakawa et al. 2004) mounted on the Subaru Telescope was used in combination with the 36-actuator AO system (Takami et al. 2004). CIAO is equipped with a 1024×1024 InSb Alladin II detector with a spatial scale of $0''.0213$ pixel^{-1}. The spatial resolution provided by the AO system was $0''.1$–$0''.2$ (FWHM), depending on the natural seeing of $0''.5$ to $1''$ at the time of the observations. The YSOs, themselves, were used as reference stars of AO, and were occulted by a mask of $0''.6$ or $0''.8$ in diameter, depending on the AO corrected PSF sizes. The masks were made of sapphire substrate coated by chromium, providing a transmittance of a few tenths of a percent. This allowed us to accurately measure the positions of the occulted stars. We used a traditional circular Lyot stop with an 80% diameter of the pupil. The throughput of the instrument, including the telescope and the AO system, is about 15%.

For obtaining an image of each object, the telescope pointing was finely adjusted so that the target star was placed at the center of the occulting mask. Three exposures of 10 s each were coadded into one frame for most cases, although the exposure time occasionally varied from 1 s to 10 s, depending on the brightness of the central star. After 24 frames of observations, both the telescope and the occulting mask were dithered by $\sim 1''$. Then, the same target was again placed at the center of the occulting mask, and 24 additional frames were taken. The total integration time for each object varied from 420 s to 1440 s. Faint standard stars (FS: Hawarden et al. 2001) were observed for photometric calibration. Dark frames and dome flat frames with incandescent lamps were taken at the end of each night.

The Image Reduction and Analysis Facility (IRAF) was used for data reduction. A dark frame was subtracted from each object frame, which was then divided by the dome-flat, and hot and bad pixels were removed. In addition to the standard data-reduction process described above, we applied the following method in order to detect any faint companions around the central bright stars. We removed the halo of the central star in each frame by subtracting the rotated image of the object, itself, rather than subtracting other PSF reference stars, since we were interested in "pointlike sources" for follow-up spectroscopy. The peak position of a PSF moved slightly on the detector during the observations, which was caused by the difference in the atmospheric dispersion between the infrared wavelength, in which the images were obtained, and the optical wavelength, in which the wavefront sensing was applied. This effect was compensated by shifting the image frame so that the peak position of each frame coincides with the frame center, after the peak position was measured with the RADPROFILE task in IRAF. Then, each object frame was rotated by 180°. The halo of the star was suppressed in each frame after the rotated image was subtracted. Finally, all of the frames for each target were combined into the final image.

We used the S-Extractor program with a 5σ detection threshold above the background in order to detect companion candidates. The background noise, dominated by the high-order asymmetry in the target star PSFs in the vicinity of the target stars, affected the source detection. We tried 32 pixels and 64 pixels as the background mesh sizes, and judged that an object was real if it was detected with both background sizes, while excluding those objects with their PSFs having ellipticities larger than 0.25 or semiminor axes smaller than 1.1 pixels.

Near-infrared spectroscopy of 26 companion candidates was carried out on 2004 December 2 to 4 with Infrared Camera and Spectrograph (IRCS) mounted on the Subaru Telescope. We used a K-band grism with a spectral resolution of R ($= \lambda/\Delta\lambda$) ~ 440 at 2.2 μm and a JH-band grism with $R \sim 120$ at 1.2 μm with a slit width of $0''.6$. The adaptive optics system was used to improve the PSF sizes to $0''.2$–$0''.9$. In the case where multiple companion candidates had been found around a YSO, we put two candidates in the slit simultaneously. In other cases, the slit was placed on a companion so as to be perpendicular to the line connecting the central star and the companion in order to minimize the contamination of light from the central star. The companions were observed at 2 slit positions with a $\sim 2''.5$ dithering to obtain sky data simultaneously, with 2 or 6 exposures made at each slit position. The integration time of each exposure was 150 s or 300 s, depending on the brightness of the companion. Dwarfs with a spectral type of A0 were used as standard stars for spectral calibration.

We used IRAF for spectral data reduction. Each dithered pair of object frames were subtracted from each other and divided by a flat field frame. We then geometrically transformed the frames to remove the curvature of the slit image caused by the grating. Wavelengths were calibrated with uncertainties of 20Å and 5Å in the JH and K bands, respectively, using the argon lamp observed at the end of each night. Companion candidate spectra were extracted from the transformed images using the APALL task. A one-dimensional spectrum for each object was constructed by integrating the spectral image where the intensity of the companion emission was more than 20% of the peak along the slit length at each wavelength. The spectrum was then normalized and combined to produce the final spectrum. After the hydrogen absorption lines in a standard star spectrum were interpolated and removed, the object spectrum was divided by the standard star spectrum, and was multiplied by a blackbody spectrum representing the standard star. For all cases, the contaminated fluxes from the central stars in the companion spectra were less than 1% of the companion fluxes, which were estimated from the K-band images taken just before the spectroscopic observations.

Table 1. Companion candidates.

Object	H mag	CIAO		HST		ΔEpoch	μ_α	μ_δ	Q	Br γ	Comment
		sepn. (″)	PA (°)	sepn. (″)	PA (°)	[yr]	[mas/yr]	[mas/yr]			
AA Tau/cc1	18.32	6.00	94.11								
BP Tau/cc1	14.89	3.00	261.28	3.05	259.26	4.09	4.5	−31.2	0.80	cont.	
BP Tau/cc2	17.13	5.45	7.84	5.34	7.19	4.09	4.5	−31.2	0.90	cont.	
DH Tau B	15.02	2.34	139.50	2.35	139.36	4.98	11.6	−24.6	0.49	cont.	
DI Tau/cc1	18.41	5.18	133.53	5.31	133.22	5.98	10.4	−20.5			
DL Tau/cc1	14.28	8.51	62.28	8.51	62.03	4.17	7.3	−21.6	0.96	cont.	[2M]04333960+2520420
FT Tau/cc1	16.43	2.54	245.14	2.57	241.93	3.99	10.8	−18.6	2.36	cont.	
GK Tau/cc1	12.46	2.52	62.28	2.51	63.64	3.93	6.9	−4.3	0.94	1.2	[RZ93]
HBC 374/cc1	19.90	5.69	234.25								
HBC 374/cc2	19.24	5.29	137.60								
HBC 397/cc1	15.52	7.21	54.54	7.20	54.57	5.96	12.7	−15.8	0.96	4.5	[MLT05] HBC397/1
HBC 397/cc2	19.46	7.23	124.41								
HBC 415/cc1	9.98	10.04	244.46	10.15	243.85	6.27	12.4	−16.2			HP Tau/G3
HBC 415/cc2	17.12	8.32	173.88								
HD 23793/cc1	13.94	5.12	226.14								
HD 27638 B/cc1	12.54	11.45	244.55						0.97	5.0	
HD 27638 B/cc2	13.29	10.96	226.72						0.80	cont.	
HD 27638 B/cc3	14.96	10.55	263.68								
HD 286556/cc1	18.21	11.69	138.99								
HD 286753/cc1	16.56	10.50	162.14								
HD 35007 B/cc1	16.08	4.48	126.74						0.93	cont.	
HD 35007 C/cc1	17.71	6.03	83.37						0.71	cont.	
HD 41593/cc1	15.88	11.10	328.40						0.85	cont.	
HDE 283572/cc1	15.87	5.68	56.06	5.63	57.28	8.36	6.5	−29.6	0.81	cont.	
HDE 283572/cc2	16.73	8.19	152.31	8.42	152.22	8.36	6.5	−29.6	0.87	cont.	
HDE 283572/cc3	17.73	6.27	16.13	6.09	16.37	8.36	6.5	−29.6	0.77	cont.	
IP Tau/cc1	15.66	3.79	124.53	3.89	124.82	4.77	5.7	−26.5			
IQ Tau/cc1	13.67	10.50	304.59	10.63	303.95	3.74	7.3	−28.8	0.97	4.9	B&C [2M]04295091+2606504
IQ Tau/cc2	13.98	10.10	302.17	10.20	301.48	3.74	7.3	−28.8	0.97	4.9	B&C [2M]04295091+2606504
IQ Tau/cc3	16.01	9.96	164.39	10.10	163.96	3.74	7.3	−28.8			
LkCa 4/cc1	12.06	8.76	155.49						0.90	cont.	[2M]04162839+2807278
LkCa 4/cc2	15.97	8.84	111.01								
LkCa 19/cc1	17.67	4.29	281.83						0.83	cont.	[MLT05] HBC 426/1
LkCa 19/cc2	20.06	5.76	293.95						0.70	cont.	
LkCa 19/cc3	13.82	11.60	323.79						0.67	cont.	[MLT05] HBC 426/2
LkCa 19/cc4	21.38	9.21	208.15						1.05	cont.	
RX J0336.0+0846/cc1	19.29	10.57	107.76						0.96	cont.	
RX J0409.8+2446/cc1	19.38	5.68	180.92								
RX J0409.8+2446/cc2	20.34	3.45	335.85								
RX J0420.8+3009/cc1	13.65	6.72	60.51								[2M]04205026+3009189
RX J0423.5+0955/cc1	13.19	1.64	356.60						0.85	cont.	
RX J0423.5+0955/cc2	20.56	6.66	306.66								
RX J0423.5+0955/cc3	17.60	10.68	257.44								
RX J0438.2+2302/cc1	13.36	9.20	94.14								[2M]04381627+2302271
RX J0445.3+0914/cc1	15.57	2.69	69.78						0.76	cont.	
RX J0445.3+0914/cc2	19.07	12.78	42.60								
RX J0512.0+1020/cc1	21.25	3.06	284.62								
RX J0512.0+1020/cc2	19.44	9.53	46.84								
RX J0528.4+1213/cc1	14.48	2.45	60.10						0.74	cont.	
RX J0528.4+1213/cc2	19.20	6.63	9.42								
RY Tau/cc1	14.81	10.83	122.41								[2M]04215810+2826300
V819 Tau/cc1	12.54	10.20	173.20	10.34	173.27	5.33	4.6	−32.6			[L93]
V827 Tau/cc1	19.16	5.13	281.05								
V830 Tau/cc1	14.71	11.27	58.46						0.92	2.7	[2M]04331073+2433493
V830 Tau/cc2	16.46	7.08	308.29						1.00	8.5	

μ_α, μ_δ: Proper motion of the central star. ΔEpoch: Interval of HST and Subaru observations.
[L93]: Leinert et al. (1993). [MLT05]: Massarotti et al. (2005). [RZ93]: Reipurth and Zinnecker (1993).

3. Results and Discussion

3.1. Photometry

Fifty-five companion candidates were detected around 33 YSOs out of 72 YSOs surveyed (table 1 and figure 1). The main purpose of this paper is to discuss the natures of 26 companion candidates based on our spectroscopic and proper-motion tests, but we start with a discussion on how many real companions are expected out of the 55 companion candidates. Figure 2 is a plot of the magnitude distribution of the companion candidates as a function of the separations from the central stars. Figure 2 shows their H-band magnitudes ranging from 10 to 21 mag with a rapid decrease in number around 20 mag. Although the completeness limit is not uniform through the survey, we may statistically assume that $H \sim 20$ mag gives a measure of the completeness limit.

The dotted line in the bottom of figure 2 represents the expected number of background stars, which was estimated from the star-count model of the Galaxy (Jones et al. 1981), which gives an average of 0.68 background stars with a limiting magnitude of $H = 20$ mag in the field of view of CIAO ($22'' \times 22''$). This figure shows that the detected number of candidates is inclined to be larger than what we expect from their random distribution, although the significance is at most at the 2σ level. From this we may infer that some of the detected candidates in our survey are not merely background stars, but are real companions. We thus conducted a proper-motion test based on the astrometry with the SDPS data and the Hubble Space Telescope (HST) archive images. If a detected object is physically associated with its central star located at the distance of the Taurus molecular cloud, the H-band magnitude of 20 mag corresponds to an object with 1 M_J at its age of

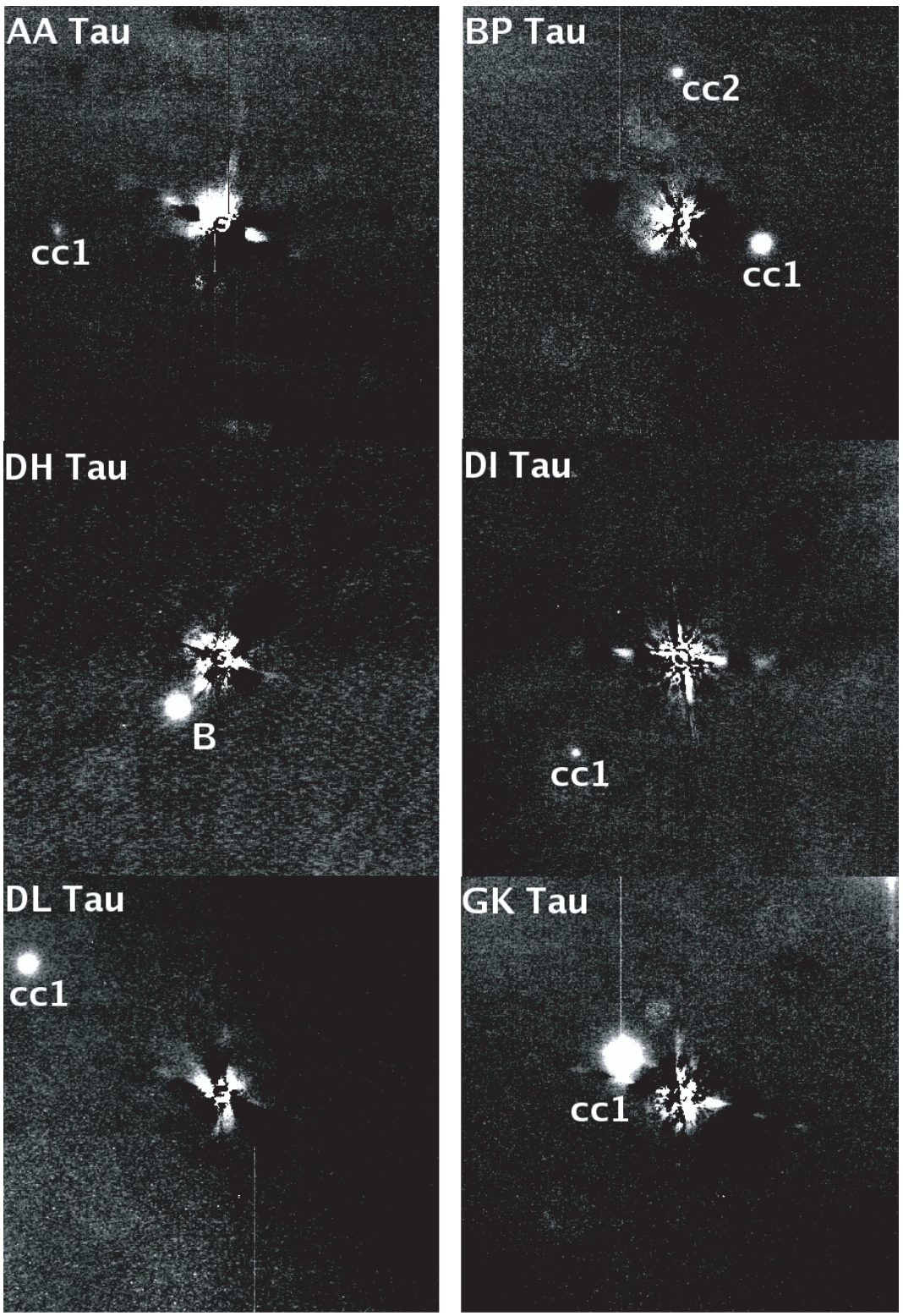

Fig. 1. H-band coronagraphic images of some faint companion candidates. The central stars are located at the center of the images, but are blocked by the mask. The halo of the central star is suppressed by subtraction of the rotated image of the object, itself. The field of view of each image is $16''\times16''$. North is up, and east is to the left.

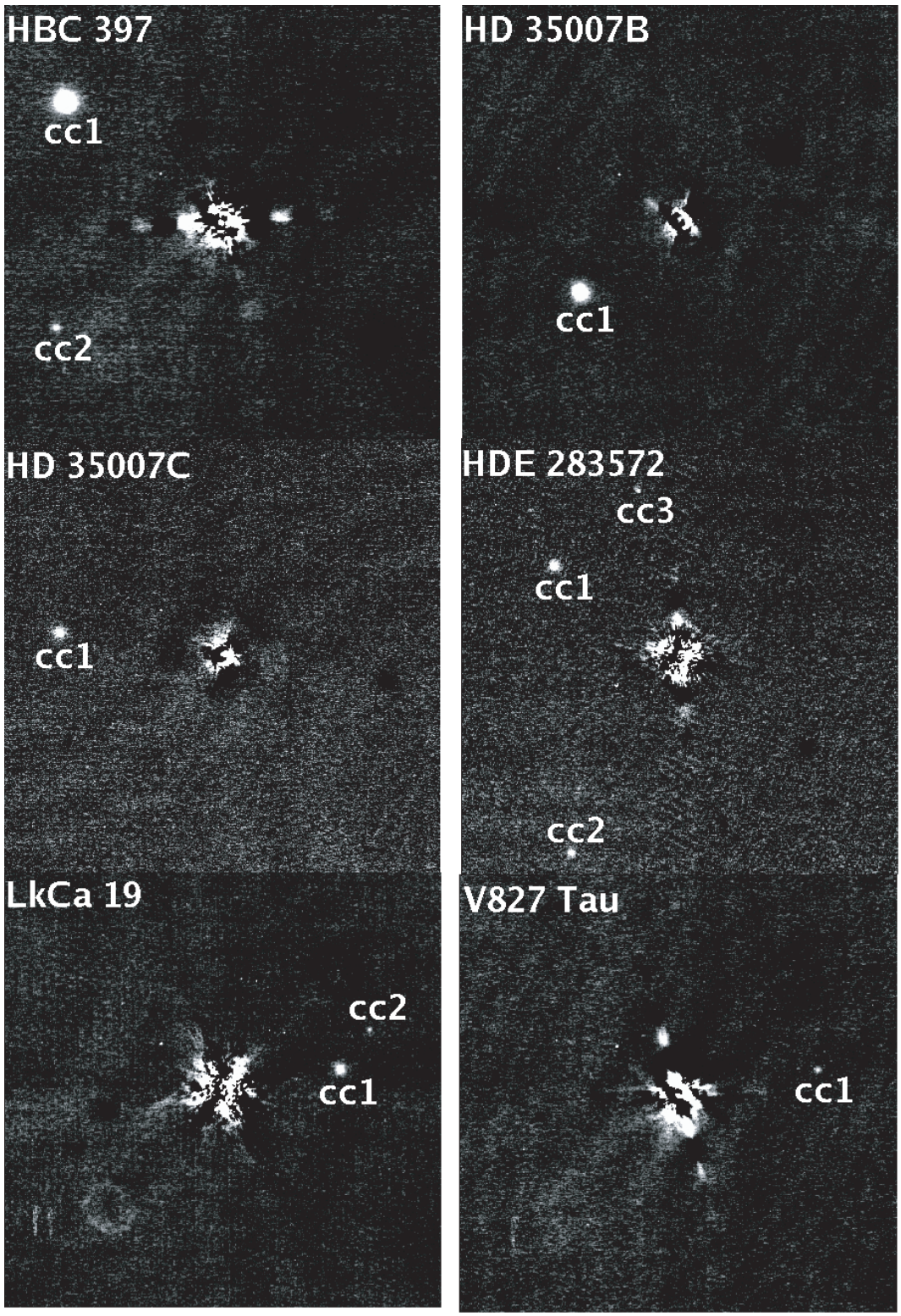

Fig. 1. (Continued.)

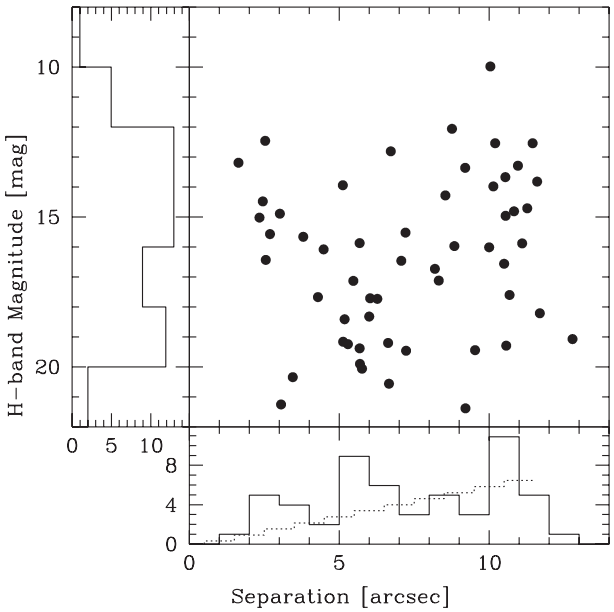

Fig. 2. Magnitude distribution of the companion candidates as a function of the separations (filled circles). The solid histograms show the magnitude and separation distributions of the companion candidates. The dotted histogram shows the expected number of background stars.

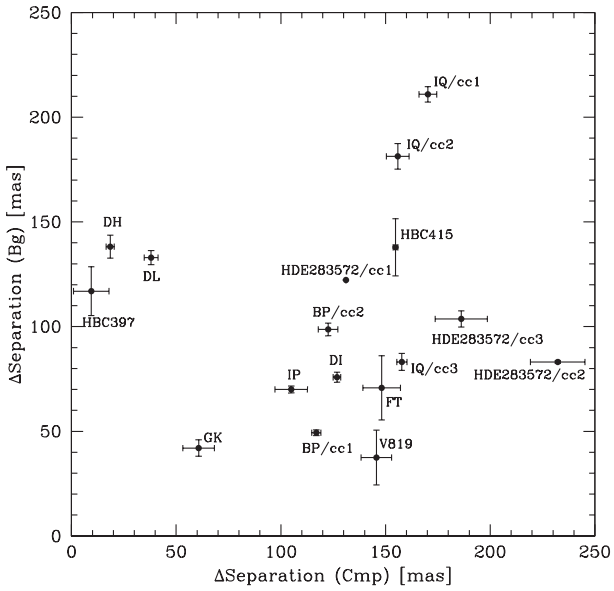

Fig. 3. Proper motion of the companion candidates. The horizontal axis shows the difference of the position of the companion candidate relative to the central star between the two observational epochs. If the candidate is a companion, the object is plotted at zero in the horizontal axis. The vertical axis represents the position difference between the two epochs minus the proper motion of the central star. If the candidate is a background star, it should be plotted at zero in the vertical axis.

1 Myr (Baraffe et al. 2003). However, we note that because such models start with assumed arbitrary initial conditions, they are very uncertain until 10 Myr (Chabrier et al. 2005).

3.2. Astrometry for Proper-Motion Test

Separations and position angles (PAs) of the companion candidates with respect to the central stars are presented in table 1. Separations and PAs are also presented in table 1 for those candidates that are also found in the HST archive data imaged during the period from 1995 to 1999. If a companion candidate is physically associated with its central star, the central star and the candidate must share a common proper motion, because the orbital motion of the assumed companion is negligible in these samples with large semimajor axes. Thus, a real companion should show no change in the separation and PA between the epochs of HST and Subaru observations. If a candidate is indeed a background star, the separation and PA should change as a result of the proper motion of the central star, because the stars associated with the Taurus molecular cloud generally show large proper motions of $\mu_\alpha = +0\farcs6$ cent.$^{-1}$ and $\mu_\delta = -2\farcs2$ cent.$^{-1}$ (Jones & Herbig 1979).

These two possibilities are tested in figure 3. The horizontal axis shows the difference in the separations of companion candidates relative to their central stars between the two observing epochs. If a companion candidate is physically associated with the central star, or it happens to have the same proper motion as the star, the object is plotted at zero in the horizontal axis. The vertical axis, on the other hand, shows the difference in the separations of companion candidates relative to their central stars between the two observing epochs after the proper motions of the central stars (Monet et al. 2003; Hanson et al. 2003[1]; Zacharias et al. 2004) are corrected. The proper motions of the companion candidate are unknown, and are not corrected. If a candidate is a background star with its proper motion being negligible, it should be plotted at zero in the vertical axis. Figure 3 shows a distinct group of three objects DH Tau B, DL Tau/cc1, and HBC 397/cc1 located near zero along the horizontal axis, indicating that these have a high possibility to be physically associated with their central stars. For the other companion candidates, the evidence of physical association is scanty.

3.3. Near-Infrared Spectra

Near-infrared spectra of the 26 companion candidates around 19 YSOs are shown in figure 4. For young, low-mass objects, we expect prominent features of Br γ (2.17 μm), CO bands (2.29 μm and longer), and H_2O absorption bands ($< 2.15\,\mu$m and $> 2.3\,\mu$m) in the K band and H_2O absorption bands in the JH band. We will examine below whether these features are detected in the observed spectra.

3.3.1. The Br γ feature

We measured the equivalent widths of the Br γ line with SPLOT task by applying a Gaussian fitting (table 1).

Six objects have a Br γ line in absorption, suggesting that they are not young and are background stars. The equivalent widths of their Br γ absorption features are 1–9Å, consistent with the spectral types of B, A, F, and G (Ali et al. 1995). The number of these background stars is consistent with the star-count model of Jones et al. (1981), which predicts 4 stars of B, A, F, or G type with $H < 20$ mag in a 2.6 arcmin^2 area (19

[1] Lick NPM2 Catalog (Strasbourg: CDS), ⟨http://vizier.cfa.harvard.edu/viz-bin/VizieR?-source=I/283A⟩.

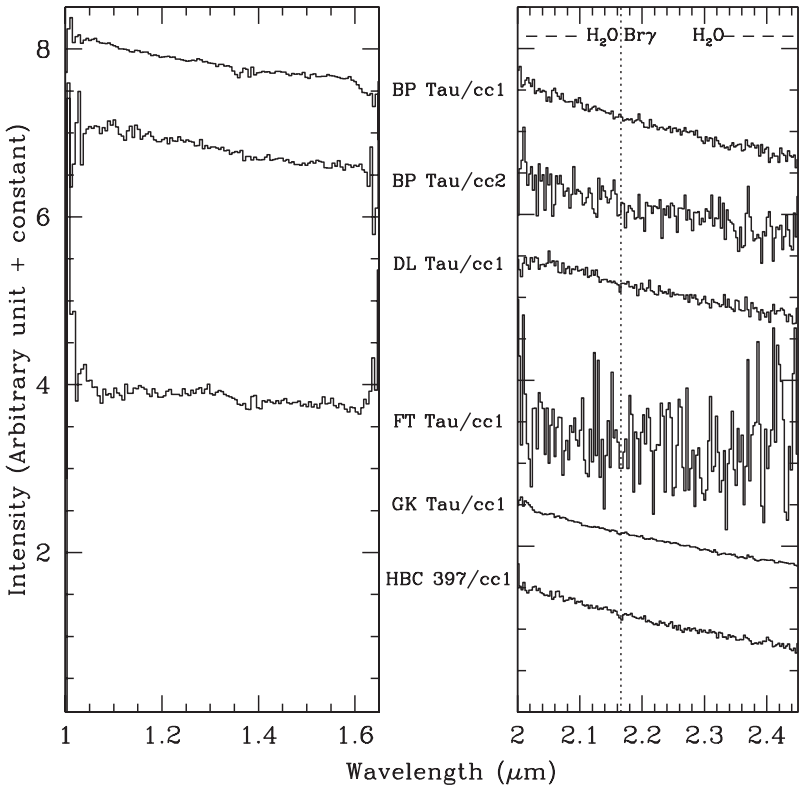

Fig. 4. (a) Near-infrared spectra of the companion candidates.

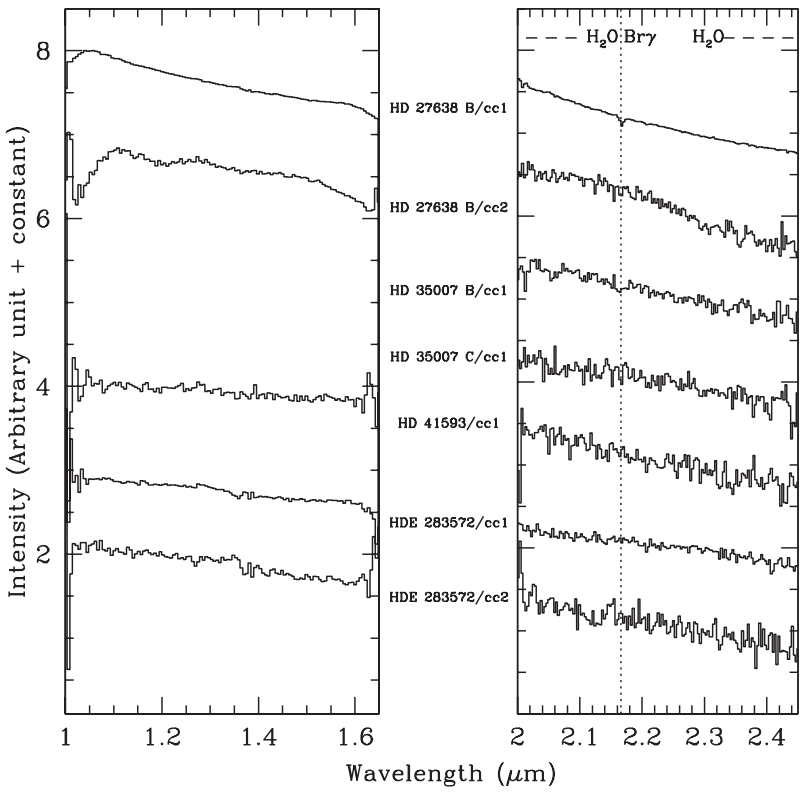

Fig. 4. (b) Near-infrared spectra of the candidates.

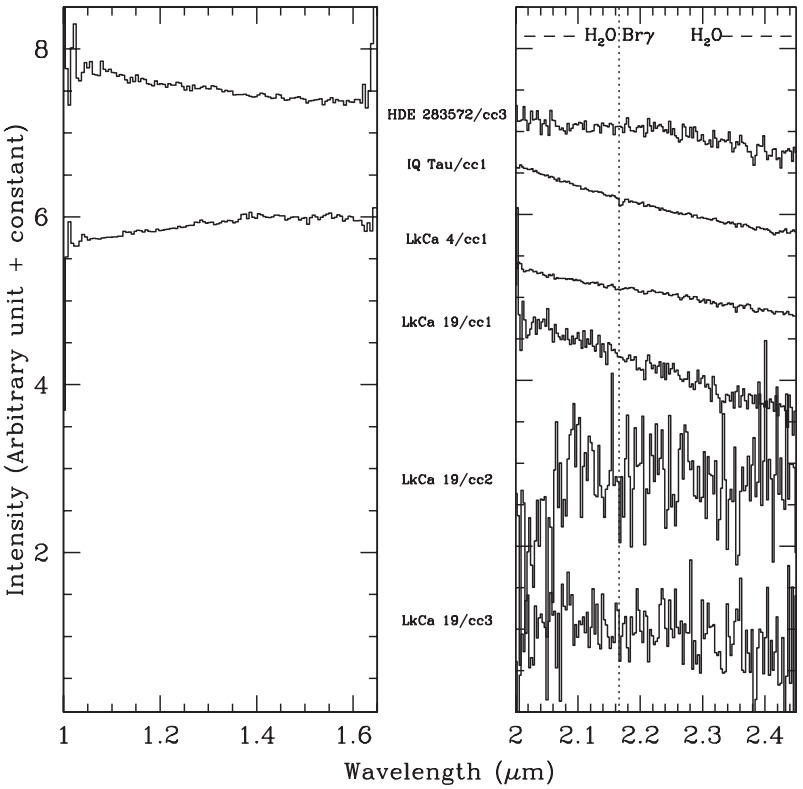

Fig. 4. (c) Near-infrared spectra of the candidates.

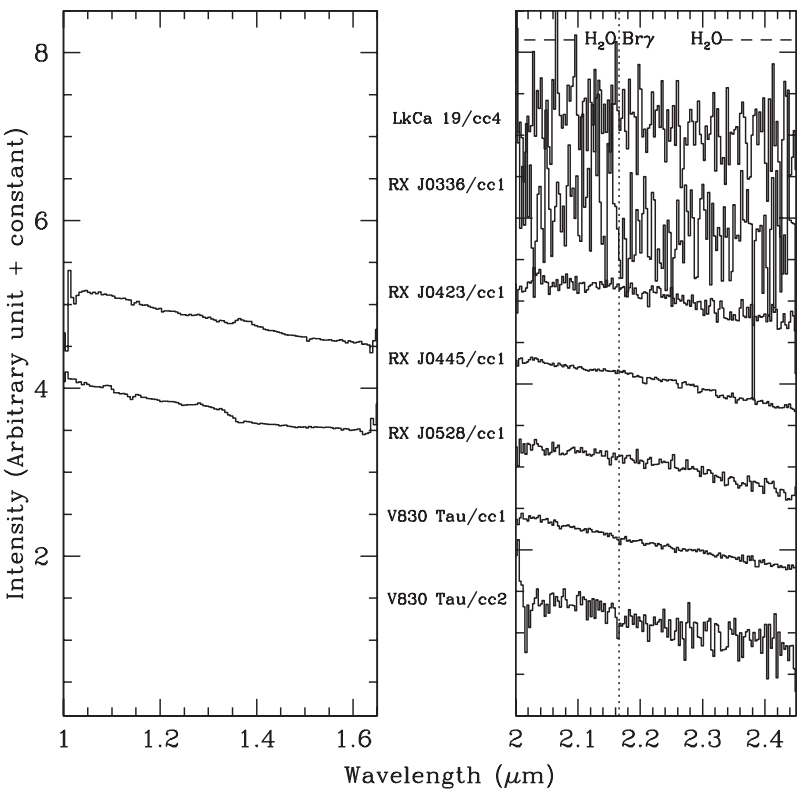

Fig. 4. (d) Near-infrared spectra of the candidates.

fields of CIAO) toward the Taurus molecular cloud.

No object was detected showing Br γ emission, and no clear evidence of youth was found for any companion candidates.

3.3.2. The H_2O absorption bands

The H_2O absorption bands in the near-infrared wavelengths are a sensitive function of the effective temperature for cool stars (Itoh et al. 2002). We calculated a reddening-independent index of the H_2O band strengths, Q, following Wilking, Greene, and Meyer (1999). With Koornneef's extinction law (Koornneef 1983), the Q index is written as

$$Q = \left(\frac{F_1}{F_2}\right)\left(\frac{F_3}{F_2}\right)^{1.41}, \quad (1)$$

where F_1, F_2, and F_3 are the flux densities in the ranges of 2.07–2.13 μm, 2.267–2.285 μm, and 2.40–2.45 μm, respectively. The Q value is close to unity for objects earlier than K type, while late M- or L-type dwarfs have a Q value as small as 0.5.

Table 1 shows that the Q values of the companion candidates are in many cases close to 1.0, suggesting that they are earlier than K type. Some objects have a Q value as low as 0.7, which corresponds to an effective temperature of 3000–4000 K.

A 1 Myr old, 8 M_J object has $H = 15$ mag with an effective temperature of $\sim$2200 K (Baraffe et al. 2003), which would have $Q \sim 0.5$. Thus, the shallow depths of the observed H_2O absorption bands imply that most of the candidates are not low-temperature planetary mass objects.

3.4. Comments on Individual Objects

3.4.1. DH Tau B

DH Tau B is claimed to be a young brown-dwarf companion of $H = 15.0$ mag located 2.″34 away from DH Tau A, as reported in a separate paper (Itoh et al. 2005). Its companionship was established by multiple proper-motion measurements. The near-infrared spectrum has deep absorption bands of water with $Q = 0.49$ as well as strong absorption lines of potassium in the J band and sodium in the K band. The spectrum is well fitted with a synthesized spectrum of $T_{\rm eff} = 2700$–2800 K and $\log g = 4.0 - 4.5$. Its mass and age are estimated to be $\sim 40 M_J$ and 10^7 yr, respectively, using the evolutionary track of Baraffe et al. (2003). Instead, if we used only the H-band photometry and assumed its age of 1 Myr, its mass can be estimated as 8 M_J, and the effective temperature would be $\sim$2200 K.

Also note that if we used the evolutionary track of Wuchterl (2005), as was the case of GQ Lup b (Neuhäuser et al. 2005), the mass would be derived as 5 M_J.

3.4.2. DL Tau/cc1

Our proper-motion measurements favor its companionship to DL Tau. The H-band magnitude is 14.3 mag, slightly brighter than that of DH Tau B. If DL Tau/cc1 is associated with DL Tau, and has the same age of 10^6 yr, its mass would be 12 M_J.

Its I-band flux estimated from the evolutionary track of Baraffe et al. (2003) is 1.6×10^{-15} W m^{-2} μm^{-1}, which is roughly consistent with the F814W-band flux of 2.3×10^{-15} W m^{-2} μm^{-1} measured with HST. However, the flux at the F675W band is 2.0×10^{-15} W m^{-2} μm^{-1}, and is $\sim$5 times larger than that estimated from the same evolutionary track.

The K-band spectrum of DL Tau/cc1 is featureless with $Q = 0.96$, indicating a relatively high-temperature object, although we expected that a far fainter companion to a low-mass star should be a low-temperature object having deep water absorption bands. The apparent spectral type of the object is early K. However, it may be too early to conclude that DL Tau/cc1 is not a low-temperature object because its near-infrared spectrum could be featureless with a large Q value if it has an active accretion disk, and the stellar photosphere is veiled. Because the ratios of metallic absorption lines are not much affected by veiling (Itoh et al. 2002) and are a good indicator of the effective temperature, moderate-to-high resolution spectroscopy to measure the equivalent widths of shallow metallic lines is being awaited.

3.4.3. HBC 397/cc1

The proper motion of this object is also similar to that of the central star HBC 397, suggestive of its real companionship. If it is associated with HBC 397 with its age of 10^6 yr, its mass would be 6 M_J. The HST flux at the F1042W band is 2.0×10^{-15} W m^{-2} μm^{-1}, consistent with the flux of a 6 M_J object calculated by using the models of Baraffe et al. (2003). Although it might be possible that heavy veiling could explain its large value of $Q = 0.96$, its K-band spectrum shows Br γ in absorption, suggesting that this object is probably a background early-type star. The apparent spectral type of the object is F. The observed flux ratio between the F1042W band and the H band, for example, is consistent with an F5-type dwarf with $A_V \sim 1.5$ mag.

4. Conclusion

A near-infrared search for faint companions around 72 YSOs in the Taurus molecular cloud was conducted as a major project of the Subaru Telescope, and 55 faint objects in the vicinity of the 33 YSOs were found. We performed near-infrared follow-up spectroscopy of 26 faint companion candidates, and conducted a proper-motion test by comparing our data with those objects that were previously imaged by HST.

Our main results are as follows:

1. We confirmed that 3 YSOs (DH Tau, DL Tau, and HBC 397) and their three faint nearby objects share common proper motions, suggesting that they are more likely to be physically associated with each other.
2. None of the near-infrared spectra of any faint objects show a deep water absorption band, except for DH Tau B, and none show the Br γ line in emission. All of them, but DH Tau B, have a high photospheric temperature or a large amount of excess from circumstellar materials.

These results indicate that the companion candidates around the two objects (DL Tau and HBC 397) with common proper motions could be young low-mass companions with heavy veiling, though we do not find clear evidence of youth.

We thank Dr. Ralph Neuhäuser for a careful reading of the manuscript and providing critical suggestions. We are grateful to S. Harasawa, H. Nakaya, T. Nagayama, and C. Nagashima for the observations. This work is partly supported by "The 21st Century COE program: The Origin and Evolution

of Planetary Systems" of the Ministry of Education, Culture, Sports, Science and Technology (MEXT), and also partly supported by a Grant-in-Aid for Scientific Research on Priority Areas "Development of Extra-Solar Planetary Science" of the MEXT. Y. I. is supported by a Grant-in-Aid for Scientific Research (No. 16740256).

References

Ali, B., Carr, J. S., DePoy, D. L., Frogel, J. A., & Sellgren, K. 1995, AJ, 110, 2415
Baraffe, I., Chabrier, G., Allard, F., & Hauschildt, P. H. 1998, A&A, 337, 403
Burrows, A., et al. 1997, ApJ, 491, 856
Chabrier, G., Baraffe, I., Allard, F., & Hauschildt, P. H. 2005, (astro-ph/0509798)
Chauvin, G., et al. 2005b, A&A, 438, L29
Chauvin, G., Lagrange, A.-M., Dumas, C., Zuckerman, B., Mouillet, D., Song, I., Beuzit, J.-L., & Lowrance, P. 2005a, A&A, 438, L25
D'Antona, F., & Mazzitelli, I. 1997, Mem. Soc. Astron. Ital., 68, 807
Hawarden, T. G., Leggett, S. K., Letawsky, M. B., Ballantyne, D. R., & Casali, M. M. 2001, MNRAS, 325, 563
Itoh, Y., et al. 2002, PASJ, 54, 963
Itoh, Y., et al. 2005, ApJ, 620, 984
Jones, B. F., & Herbig, G. H. 1979, AJ, 84, 1872
Jones, T. J., Ashley, M., Hyland, A. R., & Ruelas-Mayorga, A. 1981, MNRAS, 197, 413
Kitamura, Y., Momose, M., Yokogawa, S., Kawabe, R., Tamura, M., & Ida, S. 2002, ApJ, 581, 357
Koornneef, J. 1983, A&A, 128, 84
Leinert, Ch., Zinnecker, H., Weitzel, N., Christou, J., Ridgway, S. T., Jameson, R., Haas, M., & Lenzen, R. 1993, A&A, 278, 129
Luhman, K. L., et al. 2006, ApJ, 649, 894
Massarotti, A., Latham, D. W., Torres, G., Brown, R. A., & Oppenheimer, B. D. 2005, AJ, 129, 2294
Monet, D. G., et al. 2003, AJ, 125, 984
Murakawa, K., et al. 2004, PASJ, 56, 509
Neuhäuser, R., Guenther, E. W., Wuchterl, G., Mugrauer, M., Bedalov, A., & Hauschildt, P. H. 2005, A&A, 435, L13
Reipurth, B., & Zinnecker, H. 1993, A&A, 278, 81
Takami, H., et al. 2004 PASJ 56, 225
Tamura, M., et al. 2000, Proc. SPIE, 4008, 1153
Tsuji, T., Nakajima, T., & Yanagisawa, K. 2004, ApJ, 607, 511
Wilking, B. A., Greene, T. P., & Meyer, M. R. 1999, AJ, 117, 469
Wuchterl, G. 2005, Astron. Nachr., 326, 905
Zacharias, N., Urban S. E., Zacharias, M. I., Wycoff, G. L., Hall, D. M., Monet, D. G., & Rafferty, T. J. 2004, AJ, 127, 3043